Proc. Natl. Acad. Sci. USA
Vol. 91, pp. 9990–9994, October 1994
Plant Biology

The nodulation-signaling protein NodO from *Rhizobium leguminosarum* biovar *viciae* forms ion channels in membranes

(nodule/hemolysin/lipid bilayer/pore)

J. MARK SUTTON*, EDWARD J. A. LEA†, AND J. ALLAN DOWNIE*

*John Innes Institute, John Innes Centre, Colney Lane, Norwich NR4 7UH, United Kingdom; and †School of Biological Sciences, University of East Anglia, Norwich NR4 7TJ, United Kingdom

Communicated by Sharon R. Long, June 22, 1994 (received for review October 4, 1993)

ABSTRACT **The secreted nodulation-signaling protein NodO was purified from the supernatant of cultures of *Rhizobium leguminosarum* biovar *viciae*. The native protein has a M_r of ≈67,000, suggesting that it exists as a dimer since the DNA sequence predicts a M_r of 30,002. Pure NodO protein had no protease, pectinase, or cellulase activity, and no binding was observed to lipooligosaccharide nodulation factors. Although NodO is relatively hydrophilic, it appeared to insert into liposomes and was protected by liposomes from proteolytic cleavage. When added to planar lipid bilayers, NodO formed cation-selective channels that allowed the movement of monovalent cations (K^+ and Na^+) across the membrane. NodO is a Ca^{2+}-binding protein; in the presence of high concentrations of Ca^{2+}, channel activity was reduced. We hypothesize that NodO plays a role in nodulation signaling by stimulating uptake of nodulation factors or by forming cation-specific channels that function synergistically with the proposed lipooligosaccharide-induced depolarization of the plasma membrane of leguminous plants.**

The nodulation of leguminous plants by rhizobia depends on the bacteria making lipooligosaccharide molecules that act as specific signals recognized by legume roots (1–5). Several bacterial nodulation (*nod*) gene products essential for nodulation of legumes are involved in the synthesis of the lipooligosaccharide nodulation factors (2, 3). Different rhizobial strains make different but related signals; those from *Rhizobium meliloti* are oligomers of (three to five) *N*-acetylglucosamine residues that carry an N-linked C16:2 acyl group on the nonreducing *N*-acetylglucosamine and a sulfate group on the reducing *N*-acetylglucosamine residue (6, 7). Alfalfa root hairs deform in response to such signals at 10 pM (6), and this is accompanied by a depolarization of the root-hair plasma membrane (8). The Nod factors induce the expression of specific legume genes involved in nodule development (1, 2), and at higher concentrations the purified Nod factors can induce the formation of nodules on alfalfa even in the absence of rhizobia (5). Vetch root hairs do not respond to the *R. meliloti*-made signals but instead recognize *Rhizobium leguminosarum* biovar *viciae* nodulation factors (4), which are also oligomers of *N*-acetylglucosamine but lack a sulfate group and have different (C18:4 or C18:1) N-linked acyl groups (4).

R. leguminosarum biovar *viciae* has a nodulation gene (*nodO*) that encodes a secreted protein (9) that is involved in pea and vetch nodulation. Although mutation of *nodO* does not block nodulation, it is evident that in the absence of the *nodE* gene, *nodO* is required for the nodulation of peas or vetch (10). The *nodE* gene product is a key determinant of host specificity and introduces functional specificity into the Nod factor by causing the production of the C18:4 acyl group (4). However, NodO is not involved in the formation of the lipooligosaccharide nodulation signals, since similar signals were made by strains of *R. leguminosarum* biovar *viciae* with and without the *nodO* gene (4). Therefore, it appears that the role of NodO must be complementary to that of the lipooligosaccharide nodulation signal molecules.

The N-terminal region of NodO contains a repeated domain (9) that is similar to the Ca^{2+}-binding domain of hemolysin. Similar domains were also found in a group of secreted proteins, many of which are bacterial toxins that cause lysis of animal cells by forming cation-selective pores in the plasma membrane (11, 12). However, similar Ca^{2+}-binding domains are also found in some secreted proteases (13). To determine if NodO has any pore-forming or protease activity, we purified it and characterized it biochemically. It is evident that NodO can form pores in lipid bilayers, and we propose that it facilitates signaling by directly forming channels in plant cell plasma membranes.

MATERIALS AND METHODS

Bacterial Strains and Growth. The exopolysaccharide-deficient strains of *R. leguminosarum*, A168 and A165, with and without the symbiotic plasmid pRL1JI, have been described (14) as has been pIJ1815, which carries the cloned *nodO* gene (14). Typically, 25 ml of an overnight culture (OD_{600} ≈0.4) in TY medium (15) containing streptomycin (20 μg/ml) was inoculated into each of five 2-liter flasks containing 600 ml of the same medium containing 1 μM hesperitin to induce *nodO* expression. The cultures were shaken at 28°C for 60 h and harvested at an OD_{600} of 0.9–1.0, when the pH of the growth medium remained below pH 7.8. Normally, strain A168/pIJ1815 was used for purification of NodO, but for measurements of possible interactions between NodO and nodulation factors, NodO was purified using A165/pIJ1815. NodO isolated from either strain induced channels with similar characteristics.

Purification of NodO. All procedures were carried out at 4°C. Cells were harvested by centrifugation (9000 rpm in a Sorvall GS3 rotor for 45 min), and the culture supernatant was adjusted to pH 5.0 using glacial acetic acid and loaded at 2 ml/min onto a column (16 mm diameter) containing a 10-ml bed volume of DEAE-Sepharose Fast Flow (Pharmacia) that had been equilibrated with 0.1 M sodium acetate buffer at pH 5.0. Proteins were eluted with 0.25 M NaCl in the acetate buffer and then precipitated by adding $(NH_4)_2SO_4$ to 70% saturation. The precipitate was resuspended in 2.5 ml of 20 mM sodium acetate buffer at pH 5.0 and desalted on a PD-10 column (Pharmacia); the protein was eluted with 20 mM sodium acetate buffer at pH 5.0. Aliquots of 1.0 ml were then loaded onto a Pharmacia FPLC Mono Q column that had been equilibrated with 20 mM sodium acetate buffer at pH 5.0, and proteins were eluted at a flow rate of 1.0 ml/min using a linear gradient of 0–1.0 M NaH_2PO_4 in 20 mM sodium acetate at pH 5.0. Peak samples (fractions 23–28, Fig. 1) were

The publication costs of this article were defrayed in part by page charge payment. This article must therefore be hereby marked "*advertisement*" in accordance with 18 U.S.C. §1734 solely to indicate this fact.

pooled; the proteins were precipitated with $(NH_4)_2SO_4$ and desalted as described above, except that the proteins were eluted in a volume of 3.5 ml using a buffer containing 50 mM NaCl and 50 mM Tris·HCl at pH 7.2. One-milliliter samples were then loaded onto a Pharmacia FPLC Superose 12 column in the Tris/NaCl buffer and eluted in the same buffer at a flow rate of 0.5 ml/min. The column was calibrated with the Pharmacia low molecular weight gel-filtration kit.

Assay of NodO Insertion into Liposomes. About 1 mg of purified NodO in 0.1 M NaCl/50 mM Tris·HCl, pH 7.2, was incubated for 1 h in a final volume of 1 ml in the presence or absence of liposomes (10 mg/ml) prepared in 0.1 M NaCl/50 mM Tris·HCl, pH 7.2, as described (16). The samples were loaded onto a Pharmacia Superose 12 FPLC column equilibrated in the same buffer, and the column was eluted at 0.5 ml/min; the effluent was monitored at 280 nm. Aliquots (200 μl) of fractions corresponding to the peaks of absorbtion were assayed for the presence of NodO using a Bio-Rad SF slot-blot apparatus to transfer the samples to nitrocellulose. NodO was detected using antiserum (9) to NodO (diluted 1:1000), the bound antibody was detected using a secondary (anti-rabbit) antibody conjugated to horseradish peroxidase (Sigma), and the bound enzyme was visualized using an enhanced chemiluminescence detection kit (Amersham). Bands appearing on photographic film were scanned using a Joyce–Loebl Chromoscan 3 densitometer using arbitrary units to express the areas under the integrated peaks.

Protease Protection Assays. Liposomes (15-μl aliquots), prepared from soybean asolectin (2.5 mg/ml; type II-S; Sigma) in 1 M NaCl/5 mM $CaCl_2$/10 mM Hepes, pH 7.2, as described (16), were added to pure NodO protein (20 μg) dissolved in 20 μl of 1 M NaCl/5 mM $CaCl_2$/10 mM Hepes, pH 7.2, and incubated at 20°C for 1 h. Either trypsin (type III; Sigma) or proteinase K was then added from 20 μg/ml stocks to give a final concentration of 5 μg/ml, and the sample was incubated for 20 min at 37°C. Controls involved incubating NodO in the absence of added liposomes or adding the detergent Triton X-100 (0.1% vol/vol) to the NodO/liposome mixture prior to the addition of the protease. The samples were then boiled in SDS sample loading buffer and loaded onto a polyacrylamide gel, which was stained with Coomassie blue R250 after electrophoresis.

Conductance Measurement in Planar Membranes. Planar lipid bilayer membranes (16) were made from soybean asolectin liposomes in solutions containing NaCl or KCl with 5 mM $CaCl_2$ and 10 mM Hepes at pH 7.4. Data were collected using a CED1401 (Cambridge Electronic Design, Cambridge, UK) interfaced with an IBM personal computer and analyzed using single- and multiple-channel analysis software supplied by J. Dempster (University of Strathclyde). Bathing solution contained NaCl or KCl, and the same solution was usually present on both sides of the bilayer. Conductance values calculated from current–voltage plots were used to estimate the diameter of NodO pores according to the equation, $r^2 = Gl/\sigma\pi$, where r is the channel radius, G is the single-channel conductance, l is the estimated width of the planar bilayer (4 nm), and σ is the specific conductivity of the bathing solution. Tetrabutyl-, tetrapentyl-, tetrahexyl- and tetraoctylammonium ions (Aldrich) were prepared as 1 mM stock solutions in methanol. Ten microliters of the stock solution was added to each side of the membrane to give a final concentration of ≈10 μM. For measurements of ion selectivity, a 10-fold gradient of NaCl (0.1 M and 1.0 M) was used across the bilayer. NodO was added to the cis chamber containing 1.0 M NaCl, and a range of voltages from −200 mV to +200 mV was applied. Conductance measurements were made with single-channel recordings, and the reversal potential was estimated at zero current. Under these conditions, a perfectly selective cation pore would have a reversal potential of +59 mV. The relative permeability of Na^+ and Cl^- were calculated from the measured reversal potential of +41 mV using the Goldman–Hodgkin–Katz (17) equation.

RESULTS

Purification of NodO. The culture supernatant was passed through a DEAE-Sepharose column and eluted with 0.25 M NaCl. After precipitating the proteins from the eluate by using $(NH_4)_2SO_4$ and desalting the proteins on a PD-10 column, remaining proteins were separated on a Mono Q column. Fig. 1 *A* and *B* shows the peaks that were eluted from the Mono Q column by a phosphate gradient. The protein in the main peak (b in Fig. 1*A*) was confirmed to be NodO by using NodO antiserum and by sequencing the first 12 N-terminal amino acid residues. A peak of NodO was eluted at a higher salt concentration (peak c in Fig. 1*A*) and was contaminated with lipopolysaccharide as shown by staining with a lipopolysaccharide-specific monoclonal antibody (Fig. 1*B Right*). However, when rerun on the Mono Q column, this peak eluted at the same position as peak b in Fig. 1*A*.

The protein in peak b from the Mono Q column was then chromatographed on a Superose 12 size-fractionation column, and the native M_r of the NodO was estimated to be 67,000 (Fig. 1*C*). Since the M_r of NodO was predicted to be 30,002, based on the DNA sequence, it is likely that the native protein purifies as a dimer.

It was thought that NodO might in some way facilitate the access of lipooligosaccharide nodulation signals to the root-hair cell membranes, possibly by degrading plant cell wall components. However, extensive tests for protease activity

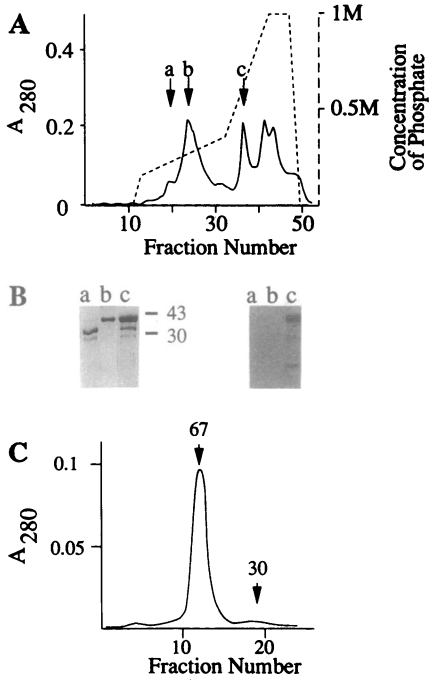

FIG. 1. Purification of NodO. (*A*) A sample of material (≈5 mg of protein) eluting from a DEAE column was desalted, loaded on a Mono Q anion-exchange column, and separated using a 0–1.0 M NaH_2PO_4 gradient in 20 mM sodium acetate buffer at pH 5.0. The effluent was monitored at 280 nm, and the major peak b corresponds to purified NodO protein. Peak c corresponds to a fraction of the NodO protein that copurified with the bacterial lipopolysaccharide, most of which eluted around fractions 40–45. (*B*) Samples a, b, and c from the Mono Q eluate were electrophoresed on an SDS/polyacrylamide gel that was stained with Coomassie blue (*Left*) or Mac114, a lipopolysaccharide-specific monoclonal antibody (*Right*) (18). (*C*) Elution of NodO from a size-fractionation Superose 12 column. NodO eluted with an apparent M_r of 67,000 (arrow labeled 67) at the same position as albumin (M_r 67,000).

using several different substrates (including casein, gelatin, and a crude pea root protein preparation) indicated that NodO (either the purified protein or crude supernatant) had no protease activity. Extensive tests for cellulase or pectinase activities were also negative. An alternative possibility was that NodO might bind to the nodulation signal molecules, but no significant binding was found between NodO and radioactively labeled lipooligosaccharide nodulation factors.

Liposomes Confer Protease Resistance to NodO. Although NodO is a relatively hydrophilic protein, it often copurified with the bacterial lipopolysaccharide (Fig. 1 and data not shown). One interpretation of this observation is that NodO might interact with the lipid domain of the lipopolysaccharide. To test if NodO associates with membranes, NodO was incubated with preformed liposomes made from the soybean lipid extract, and the mixture was loaded onto a Superose 12 size-fractionation column. Two major peaks were seen in the column elute (Fig. 2*A*); the first (at fraction 8) corresponded to the elution of the liposome fraction, and the second (fraction 12) corresponded to the elution of native NodO. Samples from each peak were quantitatively assayed for NodO using NodO antiserum. A significant amount of NodO coeluted with the liposomes (Fig. 2*A*), whereas in the absence of added liposomes (Fig. 2*B*) essentially no NodO could be detected in the corresponding fraction, indicating that NodO is incorporated into the liposomes. Such incorporation would be predicted to partially protect NodO from degradation by proteases. As shown (Fig. 3*A*), addition of the liposome preparation to NodO increased the resistance of NodO to degradation by either trypsin or proteinase K, and this resistance to degradation was lost if the detergent Triton X-100 was added to lyse the liposomes. These data indicate that NodO does interact with artificial lipid membranes and inserts into liposomes.

NodO Forms Pores in Lipid Bilayers. In addition to showing limited homology to proteases, part of NodO is homologous to the Ca^{2+}-binding domain of hemolysin and related toxins such as cyclolysin and leukotoxin. These proteins induce lysis of eukaryotic cells by forming ion channels (14). Planar lipid bilayer membranes prepared from liposome suspensions of soybean asolectin were used to test if NodO could form channels in membranes.

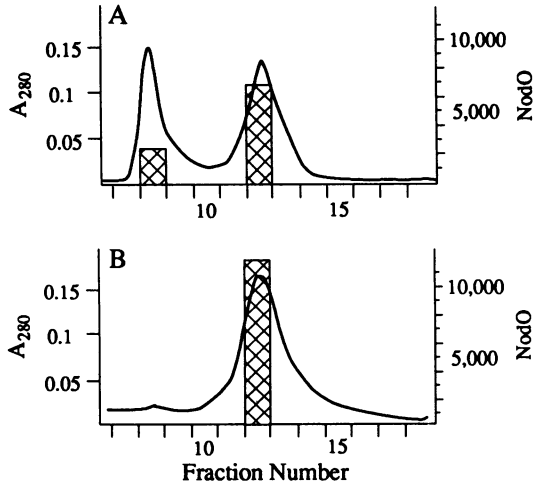

FIG. 2. Assay of NodO insertion into liposomes. (*A*) Purified NodO was incubated with liposomes, and the mixture was separated on a Superose 12 size-fractionation column. The curve shows the elution profile monitored at 280 nm. Fractions 8 and 12 were assayed immunologically for NodO by using a chemiluminescence detection system; the histograms show the relative amounts of NodO estimated by densitometry. (*B*) The conditions were as for *A* except that no liposomes were added and no NodO could be detected in fraction 8.

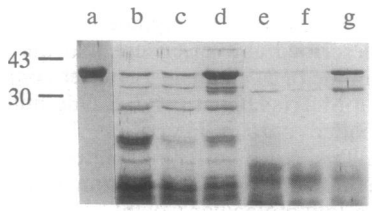

FIG. 3. Liposomes inhibit proteolysis of NodO. Purified NodO protein (lane a) was incubated in the presence of trypsin (lanes b–d) or proteinase K (lanes e–g). In lanes d and g, NodO was preincubated with liposomes, which decreased the level of proteolytic cleavage. This effect was reversed by the addition of 0.1% Triton X-100 (lanes c and f). After incubation the samples were separated by SDS/PAGE, and the gel was stained with Coomassie blue. Molecular size markers ($M_r \times 10^{-3}$) are given at left.

Highly purified NodO taken from the eluate of the Superose 12 column (Fig. 1*C*) was used for measurements of NodO-dependent current flow in lipid bilayers under voltage clamp. At concentrations between 0.1 and 1 μg/ml, NodO formed channels in membranes. Sections of typical recordings made with NodO in 1 M KCl or 1 M NaCl are shown in Fig. 4. Similar channel activity was found when NodO protein was added to either or both sides of the membrane, showing that the conductance is symmetric irrespective of any tertiary pore structure. Channel activity was seen at both low (20 mV) and high voltage (100 mV), indicating that NodO can insert spontaneously into the membrane. At higher voltage, the insertion was more frequent than at lower voltage. The conductance of channels formed by NodO showed no voltage dependence over a range of 20–200 mV. In control experiments using the control strain (A165/pIJ1518) lacking the *nodO* gene, a blank purification was followed. Fractions taken from the region where NodO normally eluted from the Mono Q column (Fig. 1*A*) or from the Superose 12 column (Fig. 1*C*) did not induce ion conductances, confirming that the pores formed were due to NodO protein and not some trace contaminant.

Typical current–voltage plots for single channels formed in 1 M NaCl or 1 M KCl solutions are shown in Fig. 5. The single-channel conductance calculated from the slopes are 1036 pS for 1 M NaCl and 1208 pS for 1 M KCl solutions in

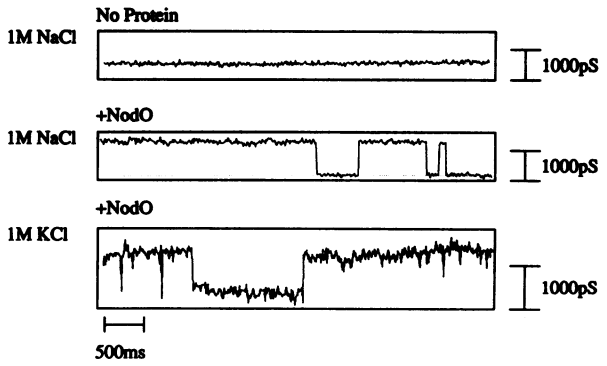

FIG. 4. NodO forms pores in lipid bilayers. Planar lipid bilayers were formed using soybean asolectin in 1 M NaCl or 1 M KCl containing 5 mM $CaCl_2$ and 10 mM Hepes at pH 7.4. NodO protein was added to one side of the bilayer, and a voltage clamp was applied. A typical current vs. time recording for an applied potential difference of 100 mV is shown. The two lower traces show channel transitions corresponding to the opening and closing of transmembrane channels formed by NodO. The unit pore size for single NodO channels is indicated for each salt solution. No changes in conductance were seen in the absence of added NodO or when a mutant strain lacking *nodO* was used as a control to identify if any other components, copurifying with NodO, could have caused pore formation.

the presence of 5 mM $CaCl_2$ and 10 mM Hepes at pH 7.4. Similar voltage-independent conductance was seen at lower salt concentrations, and calculations of single-channel conductance were made based on current–voltage plots measured at a range of different NaCl concentrations (Table 1). Taking the appropriate specific conductance values for the salt solutions used, the approximate pore diameter of the single channels formed can be calculated to be in the range of 0.78 nm to 1.23 nm (Table 1). Such calculations of pore size can give an underestimate of pore size (12, 19), and we also used a range of positively charged tetraalkylammonium ions of differing sizes, which are often used to estimate the diameter of channels formed in planar lipid bilayers (20). Such molecules, with alkyl chain lengths varying from two to eight carbons, were added after NodO-induced pores had been formed. None of these tetraalkylammonium ions blocked current flow, indicating that the pore size measured by this system may be >2 nm. Similar variations in estimates of sizes for hemolysin pores have been observed using different methods (12), and these appear to be caused by effects of ion concentrations on the pore and/or errors in the parameters used to calculate pore size from conductivity measurements (19). In addition, it is possible that the different concentrations of ions present could have a direct effect on NodO, resulting in different conductivities of the pores.

To test the ion selectivity of the channels, a 10-fold concentration difference of NaCl (1 M and 0.1 M) was set up across the membrane, and current was plotted against voltage over a range of different voltage clamps (+200 mV to −200 mV). As shown (Fig. 5, plot c) the reversal potential (the intercept of the line with the abscissa at zero current) was estimated to be +41 mV. This shows that the channel is relatively cation-selective, and when the relative selectivity is calculated (17), the pores are found to be 9.5 times more selective for Na^+ than Cl^-. Therefore NodO may play a role in the movement of cations. The requirement of Ca^{2+} for lipid bilayer formation (16) precluded measurements of Na^+ or K^+ fluxes in the absence of Ca^{2+}. Increasing the Ca^{2+} concentration from 5 mM to 100 mM caused a drop of about 30% in the overall conductance of cations through NodO pores in the membrane, indicating that the higher concentration of Ca^{2+} may induce the closure of preexisting pores.

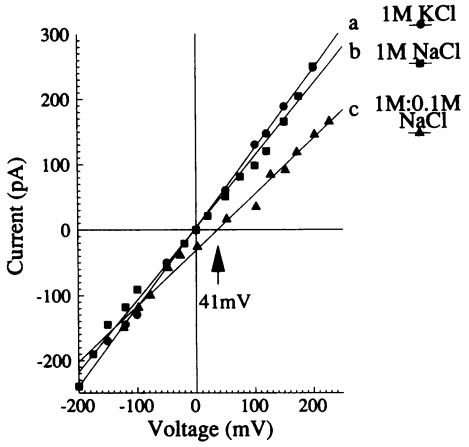

FIG. 5. Analysis of single NodO channels. Recordings of single channels formed by NodO in planar bilayers were analyzed for a range of applied potential differences between −200 mV and +200 mV under the conditions described in the legend to Fig. 4. All-points histograms were used to calculate average channel current values for each applied voltage, and the results were plotted as current vs. voltage. Each point on the graph represents an average value taken from at least 50 channel openings. Lines a and b correspond to linear regressions of data obtained using recordings made for symmetric 1 M KCl and 1 M NaCl solutions, respectively. NodO channels are symmetric with respect to the polarity of the applied voltage. The probability is <0.01 that both data sets belong to the same population. The conductance of the channels is voltage independent, allowing the conductance to be calculated as the gradient of a current–voltage plot. Thus for 1 M KCl, NodO channels have a unit conductivity of 1208 pS, whereas in 1 M NaCl the value is 1036 pS. Line c shows the current–voltage plot obtained using asymmetric salt solutions of 1.0 M to 0.1 M NaCl (1M:0.1M) when NodO was added to the cis chamber containing 1.0 M NaCl. The intercept on the abscissa gives a measure of the selectivity of NodO channels for Na^+ compared with Cl^- ions. The reversal potential of +41 mV represents a channel that is 9.5 times more selective for the cation (Na^+) than the anion (Cl^-).

Table 1. Conductance and estimated sizes of pores formed by NodO in different salt concentrations

Salt concentration	Conductance, pS	Calculated channel diameter, nm
0.1 M NaCl	320 ± 31.7	1.23
0.2 M NaCl	525 ± 53.4	1.15
0.5 M NaCl	824 ± 80.7	0.95
1.0 M NaCl	1036 ± 115.6	0.78
1.0 M KCl	1208 ± 122.5	0.85

Analysis of several multiple-channel recordings by the use of all-point histograms (Fig. 6) shows that there are several different peaks of conductance in 1 M NaCl; the principal values are 1125, 2146, and 3125 pS. The increases in conductance are in steps of about 1000 pS; each step probably corresponds to the formation of an additional channel. However, there is a series of secondary peaks of values at 1354, 2438, and 4416 pS. Again, these are separated by steps of about 1000 pS. These may represent a substrate of pores formed as a result of a different number of protein subunits or some heterogeneity in the protein monomers. However, it does appear likely that the unit conductivity of the pore (1000 pS) estimated from analysis of multiple channels is similar to that calculated from single-channel recordings.

DISCUSSION

The primary target of NodO is most likely to be at the plasma membrane of plant cells. The *R. leguminosarum* biovar *viciae*

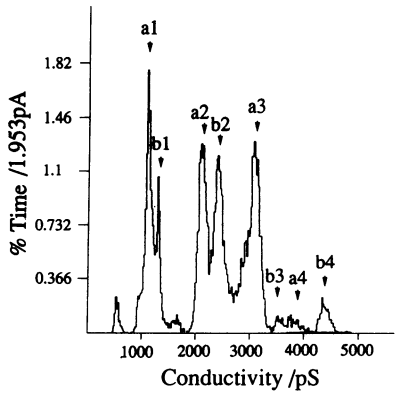

FIG. 6. Analysis of multiple channels formed by NodO. In many recordings, multiple levels of conductance were observed, presumably as a consequence of the formation of more than one NodO channel. Analysis of such recordings was carried out using all-points histograms to estimate the proportion of time spent at the different conductance levels. A typical all-point histogram is shown for a 1 M NaCl solution voltage-clamped at 100 mV. The different conductance steps presumably correspond to the opening of additional NodO channels within the bilayer. The steps between labeled peaks (a1, a2, a3, a4) give a value of about 1000 pS for the unit conductivity of the NodO pore. A second series of peaks (b1, b2, b3, b4) shows the same increases in conductance and may reflect a degree of heterogeneity in transmembrane NodO channels.

bacteria have a specialized secretion mechanism that ensures that NodO protein is secreted through both the inner and outer membranes of rhizobia: no NodO is found associated with washed, pelleted cells of *R. leguminosarum* strains producing NodO (14).

The efflux of K^+ ions across the plasma membrane of plant cells is frequently observed as a plant response to pathogen attack (21). Ehrhardt *et al.* (8) found that a purified lipooligosaccharide nodulation factor from *R. meliloti* could induce depolarization of alfalfa root-hair cells. These effects would be consistent with net cation influx, although no causal relationship has yet been demonstrated between the membrane depolarization and nodulation signaling. In the light of those observations, it is particularly interesting that the secreted nodulation-signaling protein NodO can directly form cation-selective pores in membranes. Since *R. leguminosarum* biovar *viciae* bacteria do not kill the plant cells they infect, any such movement of cations would have to be regulated to avoid cell death.

We have considered two molecular models for the role of NodO. First, given the estimated size of NodO-induced channels, they may stimulate the passage of the lipooligosaccharide nodulation factors across the plasma membrane. An alternative role for NodO might be that it induces cation fluxes across the plasma membrane in a manner that amplifies the response induced by lipooligosaccharide nodulation factors.

The requirement for NodO in nodulation is most clearly seen in *R. leguminosarum* biovar *viciae* mutants lacking *nodE* (10), a host-specific nodulation gene that encodes a protein homologous to the condensing enzyme of fatty acid synthase. Such *nodE* mutants do not make a C18:4-containing lipooligosaccharide nodulation factor, but they do make one carrying a C18:1 acyl group (4), an observation consistent with the proposed role of NodE in fatty acid biosynthesis. This latter C18:1-containing nodulation factor has significantly lowered potency in terms of induction of plant genes involved in nodule development (22) and in its ability to initiate nodule structures (4). Thus NodO may in some way compensate for the low potency of the Nod factors made by a *nodE* mutant. However, this does not necessarily mean that it does not also stimulate infection by a wild-type strain. During infection by *Rhizobium*, the majority of the infection threads are prematurely terminated. If NodO normally stimulated (but was not necessary for) infection thread growth, then loss of *nodO* might have relatively little effect on the number of nodules formed if the plant compensated for the reduced efficiency of infection by allowing more infection threads to develop to maturity. We have shown (23) that *nodO* can extend the nodulation range of a *nodE* mutant of *R. leguminosarum* biovar *trifolii*, enabling it to nodulate vetch. Thus NodO can act as a host specificity determinant for vetch nodulation even though its structure is very different from the lipooligosaccharide nodulation factors.

In some respects, NodO is analogous to hemolysin, which forms pores in red blood cell membranes (24). The characteristics of pores formed by NodO in planar lipid bilayers are similar to those formed by hemolysin; they are relatively large, have a similar conductance, and are stably open for relatively long periods of time. However hemolysin channels are voltage gated, whereas NodO channels are not. Oropeza-Wekerle *et al.* (25) demonstrated that a short synthetic oligopeptide LST-SAAAAGL (based on part of the hemolysin sequence) has hemolytic activity and also forms stable pores in lipid bilayers. This peptide has features in common with an alanine-rich potential α-helical region of NodO (FASAAAAATAI; residues 211–221). Therefore this domain of NodO might be involved in pore formation, but experimental data will be required to test this hypothesis.

The conductance characteristics of hemolysin-induced pores in red blood cells differ from those measured using lipid bilayers (26). Sublytic doses of hemolysin can cause an increase in leukotriene and histamine synthesis; this is a result of increased cellular Ca^{2+}, which activates 5′-lipoxygenase (24). In lipid bilayers, hemolysin pores have a similar closure in response to elevated Ca^{2+} (26) as that described here for NodO. In view of the similarities between NodO and hemolysin-induced pores, it is possible that NodO may function in an analogous way to hemolysin, causing an increase in intracellular Ca^{2+}, which could act as a secondary message or to stimulate the cytoskeletal changes required for infection thread growth. Such a role could be complementary to the observed depolarization of the plasma membrane of root hairs by lipooligosaccharide nodulation factors (8).

We thank S. Ghelani for technical assistance; A. Economou, T. N. H. Ellis, and A. K. Scheu for technical advice and assistance; and D. A. Hopwood and E. Schoonejans for critically reading the manuscript. We are obliged to P. Barker [Agricultural and Food Research Council (AFRC), Babraham, U.K.], who carried out N-terminal sequencing; to J. Dempster (University of Strathclyde) for providing channel analysis software; to T. Bisseling, J. Firmin, and K. Wilson for the gifts of Nod factors; and to N. Brewin for the gift of MAC114 antibody. J.M.S. was supported by a studentship from the Gatsby Charitable Foundation. This work was also supported by a grant-in-aid from the AFRC and Grant PG208/554 from the AFRC.

1. Dénarié, J., Debelle, F. & Rosenberg, C. (1992) *Annu. Rev. Microbiol.* **46**, 497–531.
2. Fisher, R. F. & Long, S. R. (1992) *Nature (London)* **357**, 655–660.
3. Spaink, H. P. (1992) *Plant Mol. Biol.* **20**, 977–986.
4. Spaink, H. P., Sheeley, D. M., Van Brussel, A. A. N., Glushka, J., York, W. S., Tak, T., Geiger, O., Kennedy, E. P., Reinhold, V. N. & Lugtenberg, B. J. J. (1991) *Nature (London)* **354**, 125–130.
5. Truchet, G., Roche, P., Lerouge, P., Vasse, J., Camut, S., de Billy, F., Prome, J.-C. & Dénarié, J. (1991) *Nature (London)* **351**, 670–673.
6. Lerouge, P., Roche, P., Faucher, C., Maillet, F., Truchet, G., Promé, J.-C. & Dénarié, J. (1990) *Nature (London)* **344**, 781–784.
7. Schultze, M., Quiclet-Sire, B., Kondorosi, E., Virelizier, H., Glushka, J. N., Endre, G., Gero, S. & Kondorosi, A. (1992) *Proc. Natl. Acad. Sci. USA* **89**, 192–196.
8. Ehrhardt, D. W., Atkinson, E. M. & Long, S. R. (1992) *Science* **256**, 998–1000.
9. Economou, A., Hamilton, W. D. O., Johnston, A. W. B. & Downie, J. A. (1990) *EMBO J.* **9**, 349–354.
10. Downie, J. A. & Surin, B. P. (1990) *Mol. Gen. Genet.* **222**, 81–86.
11. Ludwig, A., Schmid, A., Benz, R. & Goebel, W. (1991) *Mol. Gen. Genet.* **226**, 198–208.
12. Benz, R., Schmid, A., Wagner, W. Z. & Goebel, W. (1989) *Infect. Immun.* **57**, 887–895.
13. Wandersman, C. (1992) *Trends Genet.* **8**, 317–321.
14. Scheu, A. K., Economou, A., Hong, G.-F., Ghelani, S., Johnston, A. W. B. & Downie, J. A. (1992) *Mol. Microbiol.* **6**, 231–238.
15. Beringer, J. E. (1974) *J. Gen. Microbiol.* **84**, 188–198.
16. Schindler, H. (1980) *FEBS Lett.* **122**, 77–79.
17. Goldman, D. E. (1943) *J. Gen. Phys.* **27**, 37–60.
18. Sindhu, S. S., Brewin, N. J. & Kannenberg, E. L. (1990) *J. Bacteriol.* **172**, 1804–1813.
19. Jap, B. K. & Walian, P. J. (1990) *Q. Rev. Biophys.* **23**, 367–403.
20. Blaustein, R. O. & Finkelstein, A. (1990) *J. Gen. Phys.* **96**, 905–919.
21. Ranjeva, R., Thuleau, P. & Schroeder, J. I. (1993) *Curr. Opin. Biotechnol.* **4**, 172–176.
22. Horvath, B., Heidstra, R., Lados, M., Moerman, M., Spaink, H. P., Prome, J. C., van Kammen, A. & Bisseling, T. (1993) *Plant J.* **4**, 727–733.
23. Economou, A., Davies, A. E., Johnston, A. W. B. & Downie, J. A. (1994) *Microbiology* **140**, 2341–2347.
24. Welch, R. A. (1990) *Mol. Microbiol.* **5**, 521–528.
25. Oropeza-Wekerle, R.-L., Muller, S., Briand, J.-P., Benz, R., Schmid, A. & Goebel, W. (1992) *Mol. Microbiol.* **6**, 115–121.
26. Menestrina, G., Bashford, C. L. & Pasternak, C. A. (1990) *Toxicon* **28**, 477–491.